



Electrochemical immunoassay for the carcinoembryonic antigen based on the use of a glassy carbon electrode modified with an octahedral Cu₂O-gold nanocomposite and staphylococcal protein for signal amplification

Zhen Qin¹ · Wei Xu¹ · Shuai Chen¹ · Jun Chen¹ · Jing Fu Qiu¹  · Chao Rui Li¹

Received: 12 November 2017 / Accepted: 22 February 2018 / Published online: 24 April 2018
© Springer-Verlag GmbH Austria, part of Springer Nature 2018

Abstract

The authors describe an electrochemical immunoassay for ultrasensitive direct determination of the carcinoembryonic antigen (CEA). A nanocomposite consisting of octahedral Cu₂O nanocrystals covered with gold nanoparticles was utilized to modify a glassy carbon electrode which gives a strongly enhanced chronoamperometric signal for H₂O₂ which is used as an electrochemical probe. The morphology and elemental composition of the the nanocomposite was studied by field emission scanning electron microscopy and energy dispersive X-ray spectroscopy. In addition, staphylococcal protein A was placed on the electrode for efficient capture of antibody to further enhance the sensitivity of the assay. Under optimal conditions and at a typical working voltage of -0.4 V (vs. Ag/AgCl), the response covers the 2 pg·mL⁻¹ to 20 ng·mL⁻¹ CEA concentration range with a 200 fg·mL⁻¹ lower detection limit. The method was successfully applied to the determination of CEA in (spiked) human serum.

Keywords Cu₂O-Au nanocomposites · SPA · Tumor marker · Chronoamperometry · Direct method

Introduction

The carcinoembryonic antigen (CEA) is a complex glycoprotein and one of the most widely used tumor markers [1]. CEA serum levels are associated with tumor development, and CEA assays have been applied to a number of clinical questions related to the diagnosis, staging, monitoring and prognosis of cancer [2]. Therefore, a high-sensitivity and high-specificity CEA detection method for research and clinical diagnosis would be very useful.

Numerous methods for detecting CEA have been reported, such as radioimmunoassay, fluorescence measurement,

column chromatography and enzyme immunoassay, but these methods have several disadvantages, such as complex sample preprocessing and handling operations, easy contamination, high cost and long analytic time [3–6]. Electrochemical immunosensors are based on the antigen-antibody combination reaction and have been widely used in clinical diagnosis and bioassays with high selectivity and specificity [7]. Compared with other methods, electrochemical immunosensors have attracted much attention due to their advantages of high efficiency, simple operation, fast response time, miniaturization and low cost [8].

Nanomaterials have been widely used as immunosensing substrates because of their large surface area, excellent biocompatibility, excellent electrical conductivity, high receptor loading and catalytic ability [9]. Gold nanoparticles (AuNPs) are the most commonly used nanomaterial, as they not only have the characteristics of the above materials but also have good redox activity [10]. Recently, cuprous oxide (Cu₂O) nanomaterials have attracted significant attention from researchers due to their outstanding electrocatalytic performance toward H₂O₂ and have been widely applied in the immobilization of biological receptors on the surface of electrodes [11–13]. Fengyuan's group reported the use of a Cu₂O/

Electronic supplementary material The online version of this article (<https://doi.org/10.1007/s00604-018-2747-0>) contains supplementary material, which is available to authorized users.

✉ Jing Fu Qiu
jfqiu@126.com

✉ Chao Rui Li
crli@cqmu.edu.cn

¹ School of Public Health and Management, Chongqing Medical University, Chongqing 400016, China

graphene nanocomposite and its application in an electrochemical sensor for dopamine [14]. Research concerning the surface and facet-dependent catalytic properties of Cu₂O nanoparticles shows that octahedral Cu₂O nanocrystals have a larger surface area and better electrocatalytic ability than other shapes [15]. Nanocomposites doped with a noble metal show unique characteristics compared to their monometallic single metal oxide counterparts [16]. Thus, we synthesized Cu₂O-Au nanocomposites consisting of an octahedral Cu₂O nanocrystal precursor directly covered with gold nanoparticles (AuNPs), and this structure showed a further increased surface area, good stability, enhanced ability to immobilize electroactive substances and biomolecules, and excellent electrocatalytic activity toward the reduction of H₂O₂.

The immobilization of antibodies is an important factor affecting the sensitivity of immunosensors. Conventional antibody immobilization methods, such as physical adsorption and covalent bond immobilization, have low ability and efficiency to immobilize antibodies due to nonspecific adsorption and steric hindrance [17–20]. In contrast, the immobilization of antibodies using biological carriers increase the amount of immobilized antibodies [21]. Staphylococcal protein A (SPA) is a protein from the cell walls of *Staphylococcus aureus* [22]. SPA has four Fc binding domains that can specifically bind to the Fc regions of an antibody, and these properties greatly improve the antibody capture efficiency [23–27]. Hence, to further enhance the sensitivity of our sensor and reduce the analytic time, we introduce SPA as an antibody carrier.

In this work, octahedral Cu₂O-Au nanocomposites as a signal-amplifying immunosensing substrate, were first applied in an electrochemical immunosensor for the ultrasensitive direct detection of CEA. As a signal-amplifying immunosensing substrate, the Cu₂O-Au nanocomposites not only possess large surface area and high loading capacity but also display remarkable ability to catalyze H₂O₂ and excellent conductivity. Furthermore, SPA was introduced by loading on the Cu₂O-Au nanocomposites through Au-N bonds to efficiently capture anti-CEA. Experimental studies showed that this designed electrochemical immunosensor has excellent performance and exhibits high sensitivity and extraordinary specificity for the quantitative detection of CEA in human serum, showing practicability in clinical applications.

Experimental methods

Reagents and apparatus

CEA and anti-CEA were purchased from Shanghai Linc-Bio Science Co., Ltd. (Shanghai, China, <http://www.linc-bio.cn>). Recombinant staphylococcal protein A was purchased from Hangzhou Neuropeptide Biological Science and Technology Inc., Ltd. (Hangzhou, China, <http://www.nuptec.com/cn>).

Bovine serum albumin and gold (III) chloride tetrahydrate (HAuCl₄·4H₂O) were purchased from Sigma-Aldrich Chemical (USA, <http://www.sigmaaldrich.com>). Anhydrous copper (II) chloride (CuCl₂) was purchased from Sangon Biotech (Shanghai, China, <http://www.sangon.com/>). Hydrazine monohydrate (N₂H₄·H₂O, 98%) and polyvinylpyrrolidone (PVP K_{29–32}) were purchased from Aladdin. (Shanghai, China, <http://www.aladdin-e.com>). Phosphate buffered saline (PBS) containing 0.1 M Na₂HPO₄, 0.1 M KH₂PO₄ and 0.1 M KCl was used as the working buffer. All reagents were of analytical grade, and all solutions were prepared using Millipore-Q water (≥18.2 MΩ·cm).

All electrochemical measurements, including cyclic voltammetry (CV), electrochemical impedance spectroscopy (EIS) and chronoamperometry (i-t), were performed on an AUTOLAB PGSTAT302 N electrochemical workstation from Metrohm Autolab B.V. (Switzerland, <http://www.metrohm-autolab.com>). All electrochemical measurements adopted the conventional three-electrode system, using a platinum wire as the counter electrode, Ag/AgCl (with 3 M KCl) as the reference electrode and a modified 3-mm-diameter glassy carbon electrode (GCE) as the working electrode; all electrodes were purchased from Gaosunin Technology Co., Ltd. (Nanjing, China, <http://www.gaosunin.com>). Field emission scanning electron microscopy (FE-SEM) images were obtained using a Hitachi S4800 scanning electron microscope (Hitachi Limited, Japan). Energy dispersive X-ray photoelectron spectroscopy (EDS) was carried out with a VG Scientific ESCALAB 250 spectrometer (ThermoElectricity Instruments, USA). All measurements were carried out at room temperature under optimum conditions.

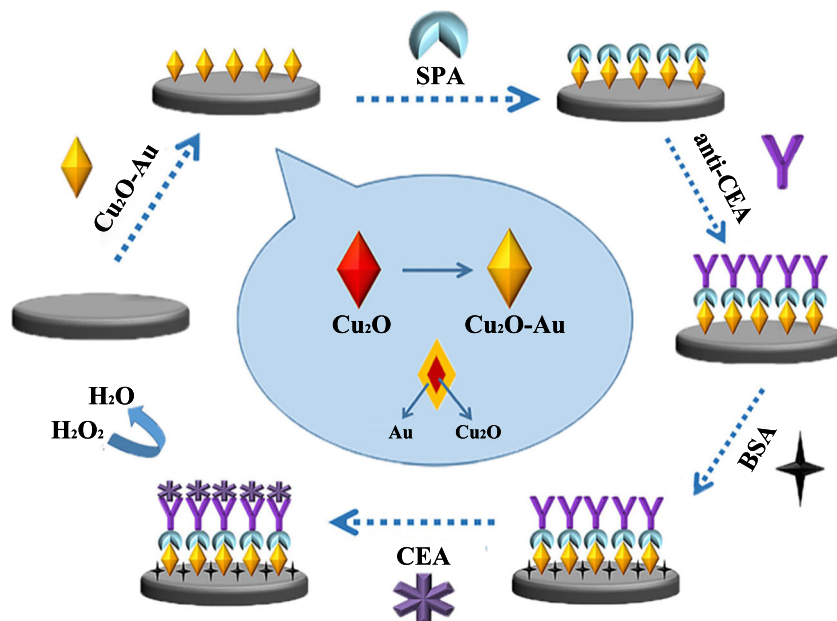
Fabrication of the electrochemical immunosensor

The fabrication procedure of the electrochemical immunosensor is outlined in Scheme 1. Prior to use, the glassy carbon electrode was polished sequentially with to a mirror with Al₂O₃ powder of 0.3 μm and 0.05 μm to a mirror. Then, the electrode were successively subjected to ultrasonic cleaning in ultrapure water and anhydrous ethanol for 5 min and allowed to dry at room temperature. Afterwards, the electrode was immersed in 0.5 M H₂SO₄ for activation under a cycling electrode potential from –1.0 to 1.0 V at a scan rate of 100 mV s^{–1} until stabilization.

Synthesis of the Cu₂O-Au nanocomposite

The octahedral Cu₂O-Au nanocomposite was synthesized following a previously reported method with minor modifications [28, 29]. 2 mg of the Cu₂O-Au nanocomposites was dispersed in 1 mL ultrapure water, and the suspension was sonicated for 30 min. The solution of the Cu₂O-Au

Scheme 1 Schematic illustration of the preparation procedure of electrochemical immunosensors for CEA



nanocomposite ($5 \mu\text{L}$, $0.2 \text{ mg}\cdot\text{mL}^{-1}$) was dropped onto the GCE surface and air-dried.

Antibody-oriented immobilization

SPA ($5 \mu\text{L}$, $3 \mu\text{g}\cdot\text{mL}^{-1}$) and anti-CEA ($5 \mu\text{L}$, $0.2 \mu\text{g}\cdot\text{mL}^{-1}$) were sequentially dropped on the Cu₂O-Au nanocomposite-modified electrodes and incubated at $37 \text{ }^\circ\text{C}$ for 1 h. Then, a BSA solution (1% , w/v) was dropped onto the modified electrodes and incubated at $37 \text{ }^\circ\text{C}$ for 1 h to block the remaining active sites and eliminate non-specific binding effects. Ultimately, CEA at different concentrations was dropped on the prepared immunosensors. The electrodes were washed with PBS after every modification step to remove unbound SPA, anti-CEA, BSA and CEA. After all the steps, the electrodes were ready for measurement.

Electrochemical measurement

All electrochemical measurements were performed in a conventional electrochemical cell using a three-electrode system at room temperature. The immunosensor was immersed in the $[\text{Fe}(\text{CN})_6]^{3-/4-}$ solution (3 mL , $5 \text{ mmol}\cdot\text{L}^{-1}$) containing 0.1 M KCl for CV and EIS analysis. CV measurements were performed at a scan rate of 100 mV s^{-1} over a voltage range of -0.2 to 0.6 V . The EIS measurements were executed with a frequency sweep from 0.1 to 10^5 Hz and a 10 mV amplitude. The immunosensor was immersed in 8 mL phosphate buffered saline (PBS) ($\text{pH } 6.4$) for chronoamperometry analysis, the amperometric $i-t$ curves were recorded at -0.4 V (vs. Ag/AgCl), $10 \mu\text{L}$, H_2O_2 solution (15% , v/v) was added to PBS

after the background current was stable, and the electrochemical signal changes were recorded.

Results and discussion

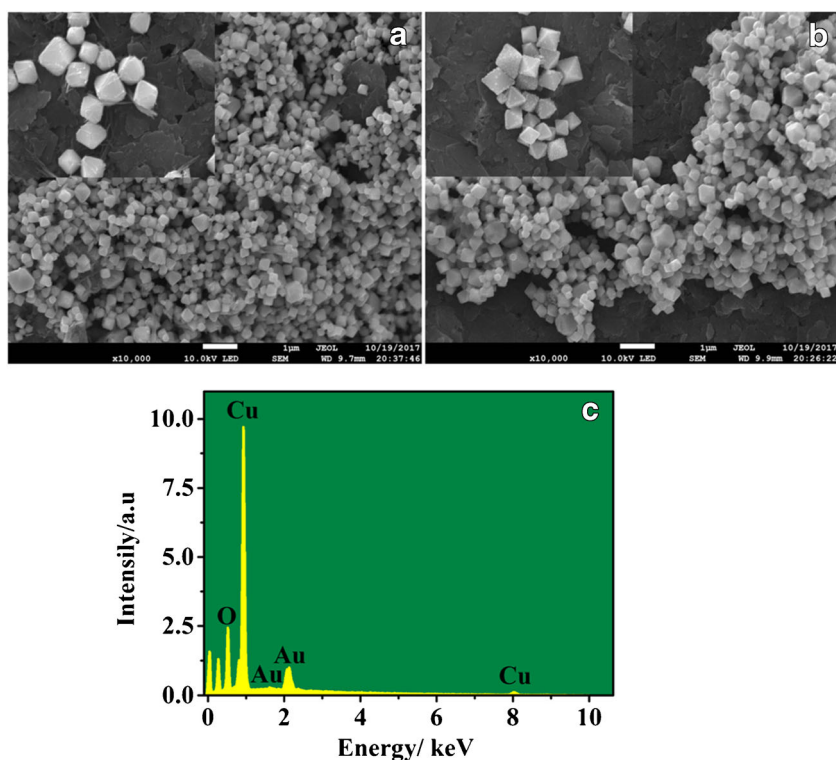
Choice of materials

In order to obtain excellent performance, the following materials were carefully selected for immunosensor construction. The octahedral Cu₂O nanocrystals were used as precursor due to their excellent electrocatalytic performance toward H_2O_2 , and the unique octahedral shape provides a larger surface area to immobilize biomolecules and better electrocatalytic ability. The Cu₂O-Au nanocomposite selected as immunosensing substrate for immobilization of SPA, by considering that metallic alloy nanomaterials have better catalytic properties than monometallic counterparts, and the strong and stable electrochemical signal in the chronoamperometry study was derived from the catalysis of H_2O_2 by the Cu₂O-Au nanocomposite. On this constructed immunosensor, SPA was adopted for oriented immobilization of antibodies to ensure antibodies being anchored on substrate surface through their Fc portion and thus the binding sites of antibodies remaining free and accessible for binding with antigens.

Characterizations of different nanomaterials

The size and morphology of the as-prepared nanomaterials were measured experimentally using FE-SEM. As Fig. 1a shows, most of the Cu₂O nanocrystals present an obvious

Fig. 1 FE-SEM image of the Cu_2O nanocrystals (**a**) and FE-SEM image of the Cu_2O -Au nanocomposites (**b**). EDS of the Cu_2O -Au nanocomposites (**c**)



octahedral shape with an average diameter of approximately 250 nm. In addition, Fig. 1b shows that the average diameter of the AuNPs is approximately 30–50 nm and that they evenly covered the surface of the octahedral Cu_2O nanocrystals. This indicates that we have successfully synthesized the Cu_2O -Au nanocomposite with an octahedral structure.

To further confirm the successful synthesis of the Cu_2O -Au nanocomposite, EDS was used to investigate the chemical composition. As seen from the EDS image (Fig. 1c), there are significant peaks corresponding to Cu_2O and Au, and agree with previous reports [28, 29]. In conclusion, these results demonstrate that the Cu_2O -Au nanocomposites were successfully synthesized.

Characterization of the stepwise-modified electrodes

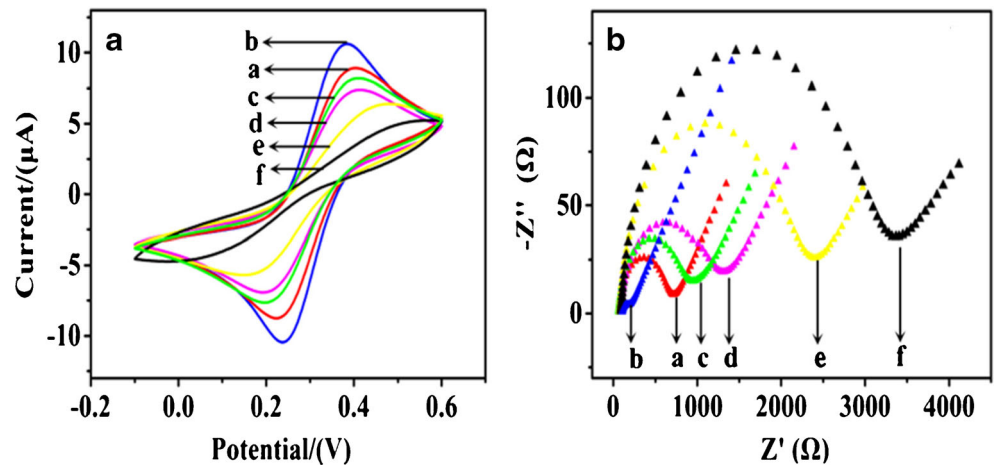
CV and EIS measurements were used to characterize the interface properties of the modified electrodes. In the CV scan of bare GCE (Fig. 2a, curve a), an obvious reversible redox peak was recorded. With the immobilization of Cu_2O -Au nanocomposites on the electrode, the redox peak visibly increased (curve b), which indicates that the Cu_2O -Au nanocomposites enhanced the effective electrochemical surface and promoted electron transfer. Then, the redox peak decreased after SPA was incubated on the immobilized electrode surface (curve c), as the non-electroactive SPA hinders electron transfer on the electrode. Next, the redox peak further declined after anti-

CEA was captured (curve d), as the non-electroactive anti-CEA further increases the resistance of the electrode surface. Similarly, when the electrode was blocked by BSA, the redox peak obviously decreased (curve e). Finally, after the addition of CEA, the redox peak was reduced to a minimum because of the high-sensitivity specific binding between anti-CEA and CEA (curve f). In addition, the EIS (Fig. 2b) results agree with the CV results. In the EIS spectra, the semicircle diameter verifies assembly, which leads to a change in the electron transfer resistance ($n = 3$). Both the CV and EIS results support the successful construction of an immunosensor.

Optimization of the experimental conditions

The sensitivity, selectivity, and electrochemical signal of immunosensors are influenced by many experimental parameters. To enhance the performance of the assay, the following parameters were optimized: (a) concentration of the Cu_2O -Au nanocomposites, (b) concentration of SPA, (c) concentration of anti-CEA, (d) incubation time for anti-CEA, and (e) pH value of the supporting electrolyte. The results are presented in the [Electronic Supporting Material](#) (Fig. S1). The following experimental conditions yielded the optimal results: (a) Cu_2O -Au nanocomposite concentration of $0.2 \mu\text{g}\cdot\text{mL}^{-1}$, (b) SPA concentration of $0.3 \mu\text{g}\cdot\text{mL}^{-1}$, (c) anti-CEA concentration of $0.2 \mu\text{g}\cdot\text{mL}^{-1}$, (d) anti-CEA incubation time of 60 min, and (e) a pH value of 6.4.

Fig. 2 **a** CV and **(b)** EIS of modified electrode recorded in 5 mM [Fe(CN)₆]^{3-/4-} solution containing 0.1 M KCl: **(a)** bare GCE, **(b)** Cu₂O-Au/GCE, **(c)** SPA/Cu₂O-Au/GCE, **(d)** anti-CEA/SPA/Cu₂O-Au/GCE, **(e)** BSA/anti-CEA/SPA/Cu₂O-Au/GCE, and **(f)** CEA/BSA/anti-CEA/SPA/Cu₂O-Au/GCE



Performance of the assay

The sensitivity and quantitative range were evaluated by amperometric *i-t* curves and quantitative detection with different concentrations of CEA under the optimal experimental conditions, at a typical working voltage of -0.4 V (vs. Ag/AgCl), the amperometric *i-t* curves were recorded by adding 10 µL of H₂O₂ (15%, *v/v*) to 8 mL PBS (pH 6.4) at 100 s. As shown in

Fig. 3a, the relationship between the electrochemical signal and the logarithmic values of the CEA concentration have strong linear relationship in the range of 2 pg·mL⁻¹ to 20 ng·mL⁻¹ with a lower detection limit of 200 fg·mL⁻¹ (based on the 3σ criterion). The regression equation is $y = -25.055 \lg C_{\text{CEA}} + 68.207$ with a correlation coefficient of $R = 0.9979$. Fig. 3b intuitively shows the relationship between the electrochemical signal with respect to the reduction of H₂O₂ and CEA

Fig. 3 **a** The linear relationship between the current response and CEA concentration ($n = 3$) in the range of 0.002–20 ng·mL⁻¹. **b** Amperometric response of the immunosensor to CEA concentrations ($n = 3$) of **(a)** 0.002 ng·mL⁻¹, **(b)** 0.005 ng·mL⁻¹, **(c)** 0.01 ng·mL⁻¹, **(d)** 0.05 ng·mL⁻¹, **(e)** 0.1 ng·mL⁻¹, **(f)** 0.5 ng·mL⁻¹, **(g)** 1 ng·mL⁻¹, **(h)** 10 ng·mL⁻¹, and **(i)** 20 ng·mL⁻¹. **c** Amperometric response to CEA (0.5 ng·mL⁻¹) compared with four nonspecific interferents including ascorbic acid (0.5 ng·mL⁻¹), uric acid (0.5 ng·mL⁻¹), dopamine (0.5 ng·mL⁻¹), tryptophan (0.5 ng·mL⁻¹), a blank sample and a mixture with above four nonspecific interferents ($n = 3$). **d** Electrochemical signal response for the detection of CEA (0.01 ng·mL⁻¹) at different weeks ($n = 3$)

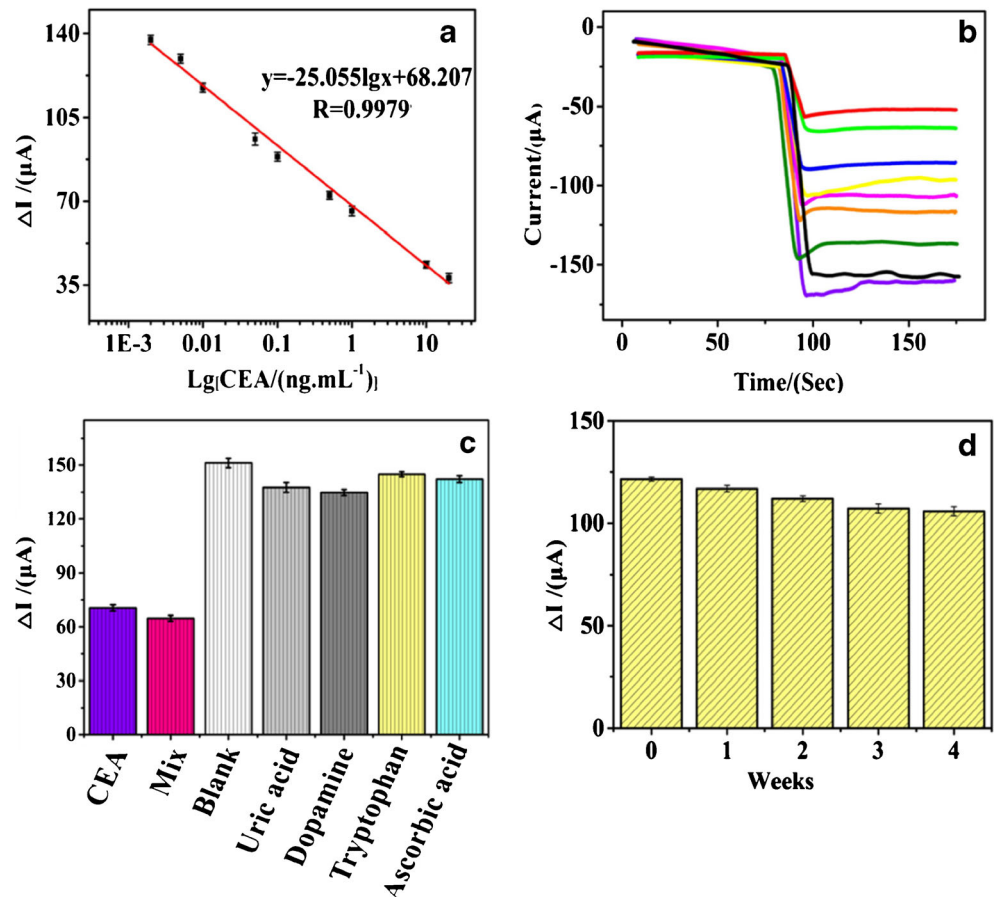


Table 1 Comparison of linearities and detection limits of the newly designed immunosensor and other CEA detection methods

| Methods | Linear dynamic range (ng·mL ⁻¹) | Limit of detection (ng·mL ⁻¹) | Reference |
|-------------------------------|---|---|-----------|
| Electrochemical immunosensing | 0.0005–5 | 0.00023 | [30] |
| Electrochemical immunosensing | 0.001–10 | 0.0007 | [31] |
| Electrochemical immunosensing | 0.02–90 | 0.02 | [32] |
| ELISA | 0.1–20 | 0.03 | [33] |
| ECL | 0.01–10.0 | 0.0038 | [34] |
| PEC | 0.01–50 | 0.0032 | [35] |
| Electrochemical immunosensor | 0.002–20 | 0.0002 | This work |

concentration. The results indicate that the electrochemical immunosensor can be used to quantitatively detect CEA. In addition, as shown in Table 1, compared with other existing CEA detection methods, the designed immunosensor has wider linear range and lower detection limit.

Specificity, stability and repeatability of the electrochemical immunosensor

High specificity, stability and repeatability of the signal response are crucial for the performance of the electrochemical immunosensor. We confirmed the specificity of the designed immunosensor by comparing the response to CEA (0.5 ng·mL⁻¹) with the response to four nonspecific interferents, such as ascorbic acid (0.5 ng·mL⁻¹), uric acid (0.5 ng·mL⁻¹), dopamine (0.5 ng·mL⁻¹), tryptophan (0.5 ng·mL⁻¹) a mixture with above four nonspecific interferents and a blank sample. As Fig. 3c shows, there was no significant difference in the responses of the blank signal and the nonspecific interferents. However, the electrochemical signal obviously changed in the presence of CEA. These results indicate the high specificity of the electrochemical immunosensor.

The stability of the immunosensor was investigated by long-term storage. The fabricated immunosensors were stored at 4 °C before testing. As seen in Fig. 3d, there were no obvious changes after the first week the signals changed less than 3.7%. After 4 weeks, the electrochemical signal retained 87.13% of the initial signal, which indicated that the immunosensor had good stability.

The reproducibility was evaluated by recording the current response of three electrodes prepared at the same concentration. As shown in the [Electronic Supporting Material](#) (Table. S1), at three different concentrations, the relative standard deviation (RSD) ranged from 1.4% to 4.8%.

Application for the analysis of the serum samples

Ten-fold-diluted human serum samples (obtained from University-Town Hospital of Chongqing Medical University) were mixed with different CEA concentrations of 0.005, 0.05, 0.5 and 10 ng·mL⁻¹, and amperometric *i*-t curves of the obtained samples were recorded. As shown in Table 2, the RSD ranged from 0.82% to 4.49%, and the recovery rates ranged from 96.8% to 104.4%.

Conclusions

In summary, an ultrasensitive electrochemical immunoassay for CEA was designed by using a signal-amplifying substrate composed of octahedral Cu₂O nanocrystals functionalized with AuNPs. On one hand, the larger surface and excellent biocompatibility of the Cu₂O-Au nanocomposite make them ideal nanocarriers to immobilize large amounts of SPA, which further enhances the antibody capture efficiency. On the other hand, the Cu₂O-Au nanocomposites have outstanding electrocatalytic activity toward the reduction of H₂O₂ and can amplify the electrochemical signal and improve the sensitivity. Due to the above advantages, the assay exhibits high

Table 2 Recovery of CEA in human serum (*n* = 3) with the proposed immunosensor

| Samples | Added CEA (ng) | Detected CEA (ng·mL ⁻¹) | RSD (%) | Recovery (%) |
|---------|----------------|-------------------------------------|---------|--------------|
| 1 | 0.005 | 0.004842 | 1.89 | 96.84 |
| 2 | 0.05 | 0.05221 | 0.82 | 104.42 |
| 3 | 0.5 | 0.5185 | 2.61 | 103.70 |
| 4 | 10 | 9.9855 | 4.49 | 99.86 |

sensitivity, good repeatability, specificity and can be used for the detection of CEA in human serum samples. We hope this electrochemical immunosensor can be considered a valid alternative for CEA determination in clinical and diagnostic applications. However, there is a limitation that the method involves several time-consuming steps led to the whole analysis takes 3.5 h, which will be addressed in future work.

Acknowledgements This research was supported by the National Natural Science Foundation of China (Grant Nos. 31071093, 31170129, and 31200064) and the Science and Technology Planning Project of Yuzhong District of Chongqing City, China (No. 20140119).

Compliance with ethical standards

The author(s) declare that they have no competing interests.

References

- Tang D, Xia B (2008) Electrochemical immunosensor and biochemical analysis for carcinoembryonic antigen in clinical diagnosis. *Microchim Acta* 163(1–2):41–48
- Hammarström S (1999) The carcinoembryonic antigen (CEA) family: structures, suggested functions and expression in normal and malignant tissues. *Semin Cancer Biol* 9(2):67–81
- Tang D, Yuan R, Chai Y, Zhong X, Liu Y, Dai J (2006) Electrochemical detection of hepatitis B surface antigen using colloidal gold nanoparticles modified by a sol–gel network interface. *Clin Biochem* 39(3):309–314
- Hasanzadeh M, Shadjou N (2017) Advanced nanomaterials for use in electrochemical and optical immunoassays of carcinoembryonic antigen. A review. *Microchim Acta* 184(2):389–414
- Dakubu S, Hale R, Lu A, Quick J, Solas D, Weinberg J (1988) Time-resolved pulsed fluorescence immunometric assays of carcinoembryonic antigen. *Clin Chem* 34(11):2337–2340
- Chu TM, Reynoso G (1972) Evaluation of a new radioimmunoassay method for carcinoembryonic antigen in plasma, with use of zirconyl phosphate gel. *Clin Chem* 18(9):918–922
- Tang J, Tang D (2015) Non-enzymatic electrochemical immunoassay using noble metal nanoparticles: a review. *Microchim Acta* 182(13–14):2077–2089
- Chikkaveeraiah BV, Bhirde AA, Morgan NY, Eden HS, Chen X (2012) Electrochemical immunosensors for detection of cancer protein biomarkers. *ACS Nano* 6(8):6546–6561
- Wang J (2012) Electrochemical biosensing based on noble metal nanoparticles. *Microchim Acta* 177(3–4):245–270
- Jia H, Yang T, Zuo Y, Wang W, Xu J, Lu L, Li P (2017) Immunosensor for α -fetoprotein based on a glassy carbon electrode modified with electrochemically deposited N-doped graphene, gold nanoparticles and chitosan. *Microchim Acta* 184(10):3747–3753
- Zhang X, Wang G, Zhang W, Wei Y, Fang B (2009) Fixture-reduce method for the synthesis of Cu₂O/MWCNTs nanocomposites and its application as enzyme-free glucose sensor. *Biosens Bioelectron* 24(11):3395–3398
- Liu M, Ru L, Wei C (2013) Graphene wrapped Cu₂O nanocubes: non-enzymatic electrochemical sensors for the detection of glucose and hydrogen peroxide with enhanced stability. *Biosensors & Bioelectronics* 45(45C):206
- Chu YG, Wang H, Ma H, Wu D, Wei Q, Du B (2016) Sandwich-type electrochemical immunosensor for ultrasensitive detection of prostate-specific antigen using palladium-doped cuprous oxide nanoparticles. *RSC Adv* 6(88):84698–84704
- Zhang F, Li Y, Gu YE, Wang Z, Wang C (2011) One-pot solvothermal synthesis of a Cu₂O/graphene nanocomposite and its application in an electrochemical sensor for dopamine. *Microchim Acta* 173(1–2):103–109
- Won YH, Stanciu LA (2012) Cu₂O and Au/Cu₂O particles: surface properties and applications in glucose sensing. *Sensors* 12(10):13019–13033
- Li F, Li Y, Feng J, Dong Y, Ping W, Lei C, Chen Z, Hui L, Qin W (2017) Ultrasensitive amperometric immunosensor for PSA detection based on Cu₂O@CeO₂-Au nanocomposites as integrated triple signal amplification strategy. *Biosens Bioelectron* 87:630–637
- Viswanathan S, Rani C, Vijay AA, Ho JA (2009) Disposable electrochemical immunosensor for carcinoembryonic antigen using ferrocene liposomes and MWCNT screen-printed electrode. *Biosens Bioelectron* 24(7):1984–1989
- Tang DQ, Zhang DJ, Tang DY, Ai H (2006) Amplification of the antigen–antibody interaction from quartz crystal microbalance immunosensors via back-filling immobilization of nanogold on biorecognition surface. *J Immunol Methods* 316(1–2):144–152
- Liu Y, Yuan R, Chai Y, Hong C, Liu K, Guan S (2009) Ultrasensitive amperometric immunosensor for the determination of carcinoembryonic antigen based on a porous chitosan and gold nanoparticles functionalized interface. *Microchim Acta* 167(3–4):217–224
- Lai W, Zhuang J, Tang J, Chen G, Tang D (2012) One-step electrochemical immunosensing for simultaneous detection of two biomarkers using thionine and ferrocene as distinguishable signal tags. *Microchim Acta* 178(3–4):357–365
- Liu N, Nie D, Tan Y, Zhao Z, Liao Y, Wang H, Sun C, Wu A (2017) An ultrasensitive amperometric immunosensor for zearalenones based on oriented antibody immobilization on a glassy carbon electrode modified with MWCNTs and AuPt nanoparticles. *Microchim Acta* 184(1):1–7
- Kessler SW (1975) Rapid isolation of antigens from cells with a staphylococcal protein A-antibody adsorbent: parameters of the interaction of antibody-antigen complexes with protein A. *J Immunol* 115(6):1617–1624
- Trilling AK, Beekwilder J, Zuilhof H (2013) Antibody orientation on biosensor surfaces: a minireview. *Analyst* 138(6):1619–1627
- Makaraviciute A, Ramanaviciene A (2013) Site-directed antibody immobilization techniques for immunosensors. *Biosens Bioelectron* 50(12):460–471
- Liu Y, Jie Y (2016) Oriented immobilization of proteins on solid supports for use in biosensors and biochips: a review. *Microchim Acta* 183(1):1–19
- Lee W, Oh BK, Min BY, Paek SH, Hong LW, Choi JW (2003) Fabrication of self-assembled protein A monolayer and its application as an immunosensor. *Biosens Bioelectron* 19(3):185–192
- Anderson GP, Jacoby MA, Ligler FS, King KD (1997) Effectiveness of protein A for antibody immobilization for a fiber optic biosensor. *Biosens Bioelectron* 12(4):329–336
- Zhu H, Du M, Yu D, Wang Y, Wang L, Zou M, Zhang M, Fu Y (2012) A new strategy for the surface-free-energy-distribution induced selective growth and controlled formation of Cu₂O-Au hierarchical heterostructures with a series of morphological evolutions. *J Mater Chem A* 1(3):919–929
- Chen S, Liu P, Su K, Li X, Qin Z, Xu W, Chen J, Li C, Qiu J (2018) Electrochemical aptasensor for thrombin using co-catalysis of hemin/G-quadruplex DNAzyme and octahedral Cu₂O-Au nanocomposites for signal amplification. *Biosens Bioelectron* 99:338–345

30. Miao L, Jiao L, Zhang J, Li H (2017) Amperometric sandwich immunoassay for the carcinoembryonic antigen using a glassy carbon electrode modified with iridium nanoparticles, polydopamine and reduced graphene oxide. *Microchim Acta* 184(1):1–7
31. Sun X, Hui N, Luo X (2017) Reagentless and label-free voltammetric immunosensor for carcinoembryonic antigen based on polyaniline nanowires grown on porous conducting polymer composite. *Microchim Acta* 184(3):889–896
32. Zhao D, Wang Y, Nie G (2016) Electrochemical immunosensor for the carcinoembryonic antigen based on a nanocomposite consisting of reduced graphene oxide, gold nanoparticles and poly(indole-6-carboxylic acid). *Microchim Acta* 183(11):1–8
33. Liu W, Guo Y, Zhao M, Li H, Zhang Z (2015) Ring-oven washing technique integrated paper-based Immunodevice for sensitive detection of cancer biomarker. *Anal Chem* 87(15):7951–7957
34. Shi GF, Cao JT, Zhang JJ, Huang KJ, Liu YM, Chen YH, Ren SW (2014) Aptasensor based on tripetalous cadmium sulfide-graphene electrochemiluminescence for the detection of carcinoembryonic antigen. *Analyst* 139(22):5827–5834
35. Han Q, Wang R, Xing B, Zhang T, Khan MS, Wu D, Wei Q (2017) Label-free photoelectrochemical immunoassay for CEA detection based on CdS sensitized WO₃@BiOI heterostructure nanocomposite. *Biosensors & Bioelectronics* 99:493